THE ASTROPHYSICAL JOURNAL, 404:316–327, 1993 February 10

A SPECTROSCOPIC AND PHOTOMETRIC STUDY OF FK COMAE IN 1989

DAVID P. HUENEMOERDER[1,2,3]
Jet Propulsion Laboratory, California Institute of Technology
LAWRENCE W. RAMSEY[2,3]
Department of Astronomy and Astrophysics, 525 Davey Laboratory, Pennsylvania State University, University Park, PA 16802
DEREK L. BUZASI[2,3,4]
Johns Hopkins University
AND
HAROLD L. NATIONS
Department of Astronomy and Astrophysics, Villanova University, Villanova, PA 19085
Received 1992 May 18; accepted 1992 August 13

ABSTRACT

FK Comae is probably a recently coalesced binary system, since it is a G-type giant rotating near breakup yet has no detected orbital motion. To better understand its characteristics, which include extreme atmospheric activity and rapid variability, an intensive spectroscopic campaign was undertaken. Fifty-one CCD-echelle spectra of this atmospherically active, rapidly rotating single giant were obtained over a period of eight nights in the spring of 1989. Visual photometry and seven *IUE* spectra were acquired contemporaneously. The photometry showed smooth quasi-sinusoidal modulation with an amplitude of about 0.1 mag. Absorption and emission lines showed complicated but systematic behavior. Photospheric absorption lines were distorted by a Doppler-shifted bump caused by dark starspots resulting in small apparent radial velocity variations. No radial velocity variations characteristic of orbital motion were seen to a level of 3 km s^{-1}. Broad emission in Hα was modulated at the photospheric rotational amplitude, implying an origin no farther from the rotational axis than 1 stellar radius. Strong absorption appears within the Balmer emission as the starspot crosses the disk. The strengths of Ca II lines are modulated in phase with Hα but do not have velocity-modulated wings like Hα. He I D3 showed very complex and interesting behavior. It had an absorption core, emission wings, and modulation with more structure than the Balmer lines. It is probably responding to the coronal X-ray flux geometric distribution. While time coverage is not as good for the UV lines, Mg II correlates well with Hα but the higher temperature lines do not.

Subject headings: stars: giant — stars: individual (FK Comae) — ultraviolet: stars

1. INTRODUCTION

FK Comae is a rapidly rotating, apparently single, G-type giant whose spectroscopic peculiarity was first noted by Merrill (1948). Optical spectra show strong, broad, and variable Hα emission (Ramsey, Nations, & Barden 1981; Walter & Basri 1982; McCarthy & Ramsey 1984). Ultraviolet spectra show chromospheric emission lines similar to those of the RS CVn binaries, only stronger (Bopp & Stencel 1981). Also like the heavily spotted RS CVn stars, FK Com displays a quasi-sinusoidal optical light curve (Dorren, Guinan, & McCook 1983; Holtzman & Nations 1984) and a high X-ray luminosity Walter (1981). As it is a member of a kinematic group, its distance, luminosity, and mass are known approximately (Eggen & Iben 1988, 1989).

The most striking peculiarity of this star is its rapid rotation for its spectral type in the apparent absence of a companion. There are two working hypotheses to explain the rapid rotation and activity. The first has a tiny yet unseen companion, dumping mass onto the visible component of FK Com, which resulted in significant angular momentum transfer (via historical orbital coupling and mass transfer) and is currently producing the atmospheric activity (Walter & Basri 1982; Walter et al. 1984). The data of McCarthy & Ramsey (1984) have made this small-companion hypothesis extremely untenable, leaving us with the alternative scenario that FK Com is a recently coalesced binary which gained its angular momentum from its once detached companion. Its atmospheric activity now is due to the strong magnetic dynamo generated by its extreme rotation rate.

Here we present the results of an observational campaign coordinated between visual photometry, optical spectroscopy, and ultraviolet spectroscopy. With these data we have examined the extent of, and correlations between, the photospheric spots, the chromospheric activity as seen in the Balmer lines, the upper chromosphere and transition region as seen in ultraviolet spectra, and even the corona, as seen in photospheric helium excited by X-rays incident from the overlying corona. We also put more stringent limits on any radial velocity variations and upon the rotational velocity.

[1] Postal address: Center for Space Research, Massachusetts Institute of Technology, Building 37-667, Cambridge, MA 02139.
[2] Visiting Astronomer, Kitt Peak National Observatory, National Optical Astronomy Observatories, which is operated by the Association of Universities for Research in Astronomy, Inc., under cooperative agreement with the National Science Foundation.
[3] Guest Observer with the *International Ultraviolet Explorer* satellite, which is sponsored and operated by the National Aeronautics and Space Administration, by the Science Research Council of the United Kingdom, and by the European Space Agency.
[4] Postal address: NASA Headquarters, Code SZ, Washington, CD 20546.

2. OBSERVATIONS

2.1. *Optical Spectra*

Optical spectra comprise the largest body of our data. They were obained at Kitt Peak National Observatory (KPNO) with the coudé feed telescope and the Penn State Fiber Optic Echelle (FOE) spectrograph in quasi-Littrow mode (QLM). This configuration gave a resolution ($\lambda/\Delta\lambda$) of 12,000 in conjunction with a 200 μm fiber and the RCA-3 CCD. The FOE/QLM images 34 orders in each spectrum, which span the wavelength range from Ca II K in the near-ultraviolet to the region of TiO λ8860 in the near-infrared. Coverage is complete in the blue and about 75% in the red. The spectrograph has been described in more detail by Ramsey & Huenemoerder (1986), and its typical data were shown by Ramsey et al. (1987) and Huenemoerder, Buzasi, & Ramsey (1989).

Spectra were extracted using local software developed specifically for fiber-optic spectra and a UNIX operating system (Rosenthal 1986). Subsequent calibrations (dispersion solution, continuum normalization) were done using the Interactive Reduction and Analysis Facility (IRAF). Due to slight mechanical flexure in the Dewar as the liquid nitrogen evaporated, flat-field images did not always align precisely with the stellar spectra. This compromised the quality of some of the near-IR orders, which are more crowded. As a result, the Ca II infrared triplet (IRT) data have increased noise.

The observing run lasted eight nights (1989 March 30–April 6), with five to seven observations of FK Com each night, along with one or more radial velocity and spectral standards. A total of 51 spectra of FK Com were acquired. Portions of each spectrum were fitted with a spectral or radial velocity standard spectrum to determine radial and rotational velocities. The continuum levels were interactively adjusted to match those of FK Com after being rotationally broadened. The root mean square (rms) deviation for four radial velocity standards observed throughout the run (totaling 22 spectra) was 0.3 km s^{-1} (0.02 pixels or roughly 0.01 resolution elements). For FK Com the accuracy is somewhat less, since its lines are extremely broadened. There were systematic deviations between different spectral orders, with an overall rms for each night of 3 km s^{-1}. The rms over all spectral orders was reduced to 1 km s^{-1} on any night when the nightly mean of the data set for each order was subtracted. The order-to-order systematic errors are apparently due to perturbations of line profiles by dark regions moving across the disk in conjunction with the distribution of line strengths in each order; this will be discussed in detail later. As a result, the best estimate of the systemic velocity is -24 ± 3 km s^{-1}, which is within the interval determined by McCarthy & Ramsey (1984). The rotational velocity, as determined from five spectral orders from each of 51 spectra, was 162.5 ± 3.5 km s^{-1}, assuming a broadening function appropriate to a rigidly rotating sphere with linear (in μ, the cosine of the angle between the line of sight and the normal to the surface) limb darkening. The optical observations log is given in Table 1.

TABLE 1

FK COMAE 1989 SPRING KPNO FOE/QLM LOG

HJD[a]	Day	Date 1989	UT	ϕ[b]
2,447,615.733.....	89.233	Mar 30	5:35:23	0.745
2,447,615.792.....	89.292	Mar 30	7:00:28	0.760
2,447,615.859.....	89.359	Mar 30	8:36:48	0.797
2,447,615.926.....	89.426	Mar 30	10:13:50	0.825
2,447,615.984.....	89.484	Mar 30	11:36:48	0.849
2,447,616.689.....	90.189	Mar 31	4:32:49	1.144
2,447,616.744.....	90.244	Mar 31	5:50:52	1.166
2,447,616.762.....	90.262	Mar 31	6:17:35	1.174
2,447,616.848.....	90.348	Mar 31	8:21:20	1.209
2,447,616.909.....	90.409	Mar 31	9:48:31	1.235
2,447,616.954.....	90.454	Mar 31	10:53:54	1.254
2,447,617.692.....	91.192	Apr 1	4:36:20	1.561
2,447,617.752.....	91.252	Apr 1	6:03:31	1.586
2,447,617.811.....	91.311	Apr 1	7:27:53	1.611
2,447,617.854.....	91.354	Apr 1	8:30:28	1.629
2,447,617.915.....	91.415	Apr 1	9:56:57	1.654
2,447,617.959.....	91.459	Apr 1	11:00:56	1.672
2,447,618.691.....	92.191	Apr 2	4:35:38	1.978
2,447,618.735.....	92.235	Apr 2	5:38:54	1.996
2,447,618.793.....	92.293	Apr 2	7:02:35	2.020
2,447,618.837.....	92.337	Apr 2	8:05:52	2.038
2,447,618.897.....	92.397	Apr 2	9:31:38	2.063
2,447,618.941.....	92.441	Apr 2	10:34:55	2.082
2,447,619.675.....	93.175	Apr 3	4:11:43	2.387
2,447,619.725.....	93.225	Apr 3	5:23:26	2.408
2,447,619.784.....	93.284	Apr 3	6:48:31	2.433
2,447,619.828.....	93.328	Apr 3	7:51:48	2.451
2,447,619.887.....	93.387	Apr 3	9:17:35	2.476
2,447,619.931.....	93.431	Apr 3	10:20:52	2.494
2,447,619.990.....	93.490	Apr 3	11:45:56	2.519
2,447,620.679.....	94.179	Apr 4	4:17:21	2.806
2,447,620.723.....	94.223	Apr 4	5:21:20	2.824
2,447,620.782.....	94.282	Apr 4	6:45:42	2.849
2,447,620.826.....	94.326	Apr 4	7:49:41	2.867
2,447,620.886.....	94.386	Apr 4	9:15:28	2.892
2,447,620.930.....	94.430	Apr 4	10:18:45	2.910
2,447,620.990.....	94.490	Apr 4	11:45:56	2.936
2,447,621.692.....	95.192	Apr 5	4:36:20	3.228
2,447,621.736.....	95.236	Apr 5	5:39:37	3.246
2,447,621.794.....	95.294	Apr 5	7:03:59	3.270
2,447,621.837.....	95.337	Apr 5	8:05:52	3.288
2,447,621.897.....	95.397	Apr 5	9:31:38	3.313
2,447,621.941.....	95.441	Apr 5	10:34:55	3.332
2,447,621.997.....	95.497	Apr 5	11:55:47	3.355
2,447,622.660.....	96.160	Apr 6	3:49:55	3.631
2,447,622.703.....	96.203	Apr 6	4:52:30	3.649
2,447,622.759.....	96.259	Apr 6	6:12:39	3.672
2,447,622.803.....	96.303	Apr 6	7:15:56	3.691
2,447,622.863.....	96.363	Apr 6	8:42:25	3.716
2,447,622.907.....	96.407	Apr 6	9:45:42	3.734
2,447,622.964.....	96.464	Apr 6	11:07:58	3.758

[a] Times given are all at the start of 3600 s exposures.

[b] A rotation-number ordinate has been added to the phase to clarify the continuity in phase of the observations.

To aid simultaneous visual examination of a large number of spectra, the data were interpolated linearly in rotational phase and stacked into a two-dimensional "spectral-phase image," in which the abscissa is wavelength and the ordinate is rotational phase. We thus essentially have the equivalent of a spectrum which has been trailed through one rotation (though we have in fact covered almost four rotations discontinuously). In such images, features which are coherent with phase are easily seen, much more so than in collections of line plots or even in an animated line plot. As a further aid in analyzing the activity, we will often subtract a model spectrum, which has been derived from the spectrum of an inactive spectral standard suitably rotationally broadened and velocity-shifted. This type of spectral data will be referred to as "subtracted" or as "excess" when referring to line strengths. The standard star used was ϵ Virginis (of spectral type G8 III), whose rotational broadening

TABLE 2

FK COMAE 1989 SPRING *IUE* LOG

Image[a]	Exposure Time (Minutes)	Day	UT	ϕ[b]
LWP 15260	5	87.986	23:40	0.225
LWP 15270	2	89.029	0:42	0.660
LWP 15275	2	90.003	0:04	1.065
LWP 15282	5	91.581	13:56	1.723
LWP 15299	5	93.642	15:25	2.582
LWP 15301	2	93.897	21:32	2.688
LWP 15302	2	93.922	22:08	2.719
LWP 15735	2	166.770	18:29	33.052
LWP 15740	2	167.742	17:49	33.457
LWP 15745	2	167.999	23:59	33.564
LWP 15746	2	168.763	18:19	33.882
LWP 15749	2	169.712	17:56	34.292
SWP 35883.....	120	88.035	0:50	0.245
SWP 35884.....	31	88.107	2:34	0.275
SWP 35894.....	120	89.075	1:48	0.679
SWP 35899.....	155	90.064	1:32	1.091
SWP 35909.....	120	91.634	15:13	1.745
SWP 35924.....	100	93.651	15:37	2.585
SWP 35928.....	80	93.974	23:22	2.720
SWP 36513.....	120	166.829	19:54	33.076
SWP 36529.....	172	167.808	19:24	33.484
SWP 36543.....	140	168.818	19:38	33.905
SWP 36549.....	164	169.810	19:27	34.318

[a] All observations were in low-dispersion mode.

[b] A rotation-number ordinate has been added to the phase to clarify the gap between early and late observations and discontinuity of phase coverage.

was unresolved. Other estimates put FK Com closer to type G0 III, but for differential comparisons G8 III is adequate.

2.2. *Ultraviolet Spectra*

Ultraviolet spectra were obtained with the *International Ultraviolet Explorer* (*IUE*). Seven each of LWP and SWP spectra were collected contemporaneously with the KPNO observations. Five LWP and four SWP spectra were made 70 days (29 rotations) later. These spectra were reduced with the standard *IUE* processing software, converted to FITS format, and line strengths were measured with IRAF's "splot" tools. The log of *IUE* observations is given in Table 2.

2.3. *Photometry*

Photoelectric photometry in the *B* and *V* bands was obtained concurrently with the KPNO spectroscopy using the Phoenix-10 automatic photoelectric telescope (APT) operated by the Automatic Photoelectric Telescope Service on Mount Hopkins (Genet et al. 1987). As the amplitudes in both *B* and *V* were so similar that little information on the starspot temperatures could be obtained from them, only the *V* data will be considered in what follows. Figure 1 shows the differential *V* photometry of FK Com for the entire 1989 observing season. As can be seen in the figure, the amplitude of the starspot modulation increased substantially as the season progressed, with both the maximum and minimum light becoming more extreme while the mean light level remained nearly constant. This emphasizes the importance of intense coordinated observations during short time periods.

Because the light curve seemed to be evolving relatively slowly near the epoch of the optical spectroscopy (JD 2,447,615 to JD 2,447,623), data in the interval 1989 March 19–April 18 (JD 2,447,604 to JD 2,447,635) has been chosen as being indicative of the state of FK Com's photosphere for that epoch. To estimate the area and distribution of the starspots on FK Com, the variability has been modeled using an implementation by Budding & Zeilik (1987) of an algorithm developed by Budding (1977). The starspots in this model are constrained to be circular in outline and to all be of the same temperature. The initial free parameters to the least-squares fit can include the inclination, *i*, of the stellar rotation axis to the line of sight; the stellar latitude and longitude of each spot center; the

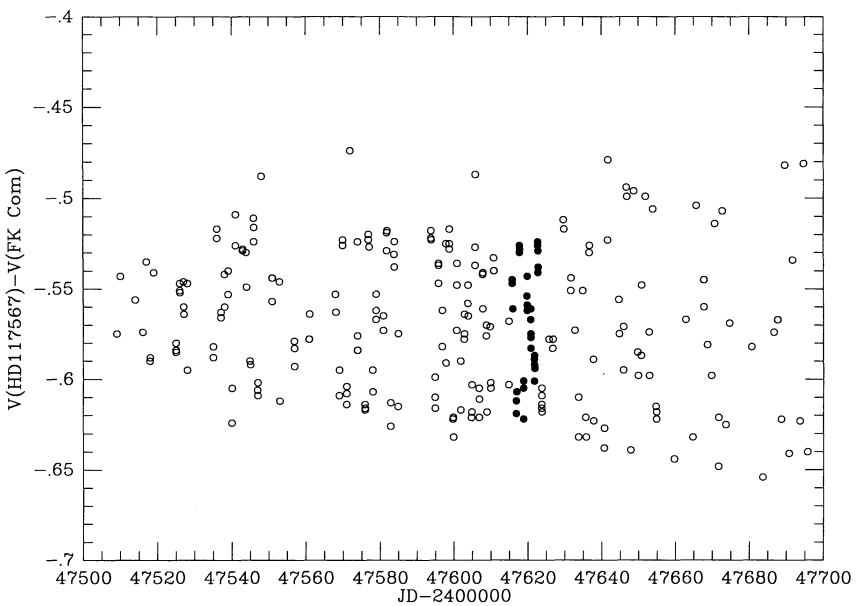

FIG. 1.—*V*-band differential photometry of FK Com (relative to HD 117567) for the 1989 observing season is shown vs. time. As the data are plotted in the sense comparison star *minus* variable, the variable is brighter at the top of the plot. The optical spectroscopy was done in the interval of JD 2,447,615–JD 2,447,623. Photometric points in this interval are shown as filled circles. The gradual change in the maximum and minimum light emphasizes the need for intensive multiband monitoring.

angular radius of each spot; the unspotted intensity to the observed light maximum, and the temperature difference, ΔT, between the spots and the unspotted photosphere. For the purposes of photometric modeling, we have chosen 60° to be a not unreasonable value and held i constant at this during the modeling. (The very high $v \sin i$ observed ensures that i cannot be a great deal less than this, because, if it were, the equatorial rotational velocity would be greater than the breakup velocity.) The temperature difference was held constant at $\Delta T = 600$ K, as found from a previous multiwavelength photometric study by Holtzman & Nations (1984). The data have been normalized to a maximum brightness as observed in APT data for the 1991 season when the difference between the comparison and variable V magnitudes was only -0.44 (H. L. Nations, unpublished data).

Since the phased light curve is very nearly sinusoidal (Fig. 2*a*), it has been fitted with a single spot model varying the geometrical parameters as discussed above. The ephemeris used here is that of Chugainov (1976) (2,442,192.345 + 2.400E).

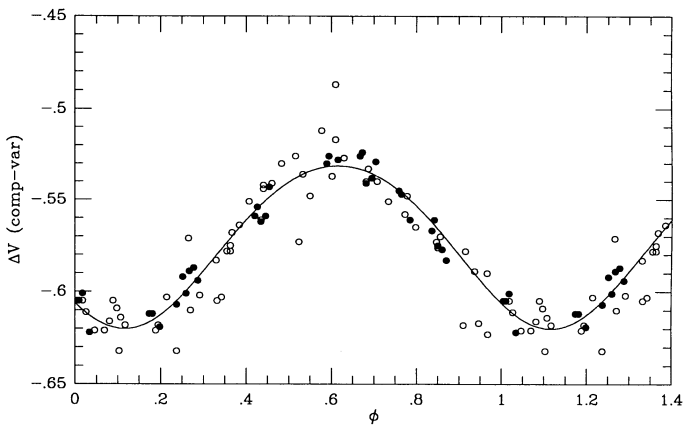

FIG. 2*a*

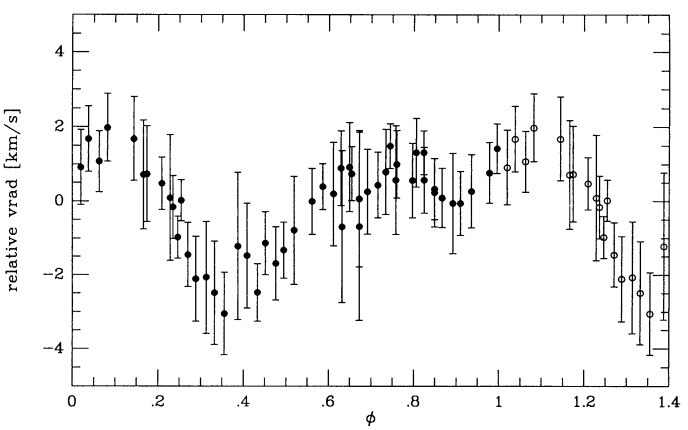

FIG. 2*b*

FIG. 2.—(*a*) Visual light curve is shown in the sense comparison *minus* variable magnitudes. Points contemporaneous with the optical spectra are shown as solid circles, while those made within 30 days are open circles. The ephemeris used is that of Chugainov (1976): 2,442,192.345 + 2.400E. The solid line is a spot model-fit light curve for a 40° radius spot at a latitude of 80°. (*b*) Relative radial velocities are plotted vs. rotational phase. One standard deviation error bars are shown. Open circles are repeated points to show continuity. While variations are real, they are not sinusoidal, and are attributed to perturbation of line profiles by dark spots.

The best fit resulted in a spot with a radius of 41°.0 ± 0°.5 located at longitude 41°.6 ± 0°.2 (or centered on the meridian at $\phi = 0.12$) and latitude 80°.3 ± 2°.7. The average error of the fit is 0.0079 (1 standard deviation), which is essentially the same as the data precision found from the comparison-minus-standard star photometric measures. This spot model is nonunique and is intended to give a sense of the scale of the spot coverage. The maximum light level likely does not represent an unspotted surface. This maximum could equally well be lowered by a longitudinally uniform distribution of spots at low latitudes instead of a single large spot at high latitudes. What the circular-spot models do measure is the asymmetry in the spot distribution.

3. DISCUSSION

3.1. *Radial and Rotational Velocities*

The radial velocity variation, or lack thereof, of FK Com is of interest, since it is directly related to the origin of the extreme rotation rate. McCarthy & Ramsey (1984) did an in depth study based primarily on the Na D lines. They were able to limit any variation to 5 km s^{-1}, and thereby put rather extreme limits on the mass of a hypothetical companion. We have found the Na D lines to be unreliable in our data, probably because of the bright Tucson sky in that band. Excluding that order, and scaling the remaining orders to a common mean, the nightly rms was found to be 1 km s^{-1}. The larger order-to-order systematic differences are presumed due to the spottedness of FK Com and perturbations of absorption-line profiles as the spotted regions move across the disk. The variance of these differences depends in a complicated way on the relative line strengths, spectral line densities, and line sensitivities to temperature in each order. A detailed analysis of spectral-phase images in these orders revealed bumps in the cores of some lines which can be traced in velocity with rotational phase. They are consistent with sinusoidal variation such as would be due to a point on the equator. The bumps become visible near minimum brightness and vanish near maximum brightness. It is difficult to trace the features in detail, but the behavior is consistent with the bumps being caused by equatorial dark spots Doppler-imaged into the line profile. For an idealized case of a single, circular, equatorial spot, we might expect the bumps to appear somewhat before minimum light. However, it is unlikely that the geometry is so simple, and, futhermore, there is the added uncertainty that the light-curve variations in active stars may be due not solely to dark spots but also to bright plage (Dorren & Guinan 1990). The apparent shift between the light-curve and wisp features is likely further evidence of this. Better (higher signal-to-noise) Doppler imaging data coupled with contemporaneous light curves could unambiguously answer this question.

The arbitrarily offset radial velocities are shown in Figure 2*b*. These data are the combined measurements of eight echelle orders for 51 spectra. It is clear that there are variations from night to night, but it is also clear that the variations are not sinusoidal. We attribute the variations to the distortion of line profiles by the Doppler imaging of spots. Determining whether there is a residual low-amplitude sinusoidal component hidden here will require detailed modeling utilizing a light curve and individual profiles rather than an ensemble average. In any event, it is obvious that the semiamplitude of any sinusoidal variation, such as would be caused by a companion in a circular orbit, is less than about 3 km s^{-1}. This makes any purport-

ed companion an even more bizarre object, and perhaps more unlikely, than that described by McCarthy & Ramsey (1984).

The projected rotational velocity found from fits to photospheric absorption lines is $v \sin i = 162.5 \pm 3.5$ km s^{-1}. There have been other estimates of the rotational velocity, which have ranged from 120 ± 20 (Bopp & Stencel 1981) to over 200 km s^{-1} (Walter et al. 1984). The value given here, however, is based on a large ensemble of photospheric absorption lines, and hence is of much greater accuracy. Given a rotational period of 2.4 days, this translates into a radius (times sin i) of $7.7 \pm 0.2\ R_\odot$. Because FK Com is a member of the HR 1614 old disk aggregate, its mass is probably near $1.5\ M_\odot$ (Eggen & Iben 1988, 1989). Thus the circular, or breakup, rate is $(\sin i)^{1/2} \times 193$ km s^{-1}; the inclination must therefore be greater than 45°. The major point to note is that FK Com is essentially rotating at the breakup velocity.

3.2. *Balmer Lines*

The Hα line of FK Com has long been noted as exceptional for stars of this spectral type; it is strong, double-peaked, and highly variable (Merrill 1948; Ramsey et al. 1981; Walter & Basri 1982). Walter & Basri (1982) noted the extreme width of the line and the regular variation of the centroid with an amplitude equivalent to the rotational velocity (which they determined to be 110 km s^{-1}) at the 2.4 day photometric period. Such is confirmed in our data, but with greater precision and accuracy. All the Balmer lines observed with sufficient signal-to-noise ratio (Hα, Hβ, Hγ, Hδ) showed excess emission, though only Hα had emission above the local continuum in the unsubtracted spectra.

The spectral-phase image of the subtraced Hα profiles is shown in Figure 3. The quasi-sinusoidal variation of the envelope is clear. It is commensurate with the photometric period and has an amplitude essentially equal to the projected rotational velocity, but not as accurately determined because of sporadic fluctuations in the profile. The extreme width of the profile is also evident, exceeding 1000 km s^{-1}. Sample subtracted profiles are shown as line plots in Figure 4. At some phases the shape is essentially Gaussian, with a dispersion of 314 km s^{-1} (or a FWHM of 740 km s^{-1}). If the profile is interpreted as a combination of a thermal profile at 10,000 K and a turbulent component, the turbulent velocity is 444 km s^{-1}. Profiles at other phases have one or both wings of this Gaussian profile, but deviate elsewhere. In fact, simply shifting the Gaussian fit at $\phi = 0.144$ by the phased projected rotational velocity matches the wings of the subtracted profiles well, as can be seen by insepection of the solid and dotted lines in Figure 4.

The strengths of Hα excess profiles are shown in Figure 5. Since we are dealing with continuum-normalized spectra, there could be apparent variations in Hα even if the Hα emission were constant, owing to the continuum variations. However, the amplitude of the photometric variations is substantially less than that of Hα, and we will not bother to correct for the continuum variations. Hα has strongest emission at minimum photometric brightness. Discontinuities in these data, as seen at $\phi = 0.9$, represent intrinsic variations occurring from one rotation to the next.

The Hα excess centroid varies sinusoidally with phase, just as was seen in the wings in Figure 3, indicative of a common origin for the wing emission and the bulk of the emission. The peak-to-peak amplitude in the centroid is about $2.2v \sin i$. There is a slight phase-lead of about 0.1 in the centroid relative to the strength; the line becomes most blueshifted before the minimum strength. The overall form of the variation of the centroid with phase strongly resembles that of the strength, including the discontinuities seen in the latter.

While the Hβ line is not as strong as Hα, its wings, centroid, and strength vary in phase similarly to those of Hα. The spectral-phase image of the excess Hβ is shown in Figure 6. Velocity modulation of the wings is apparent here, too. However, strong excess absorption is visible as the black blob

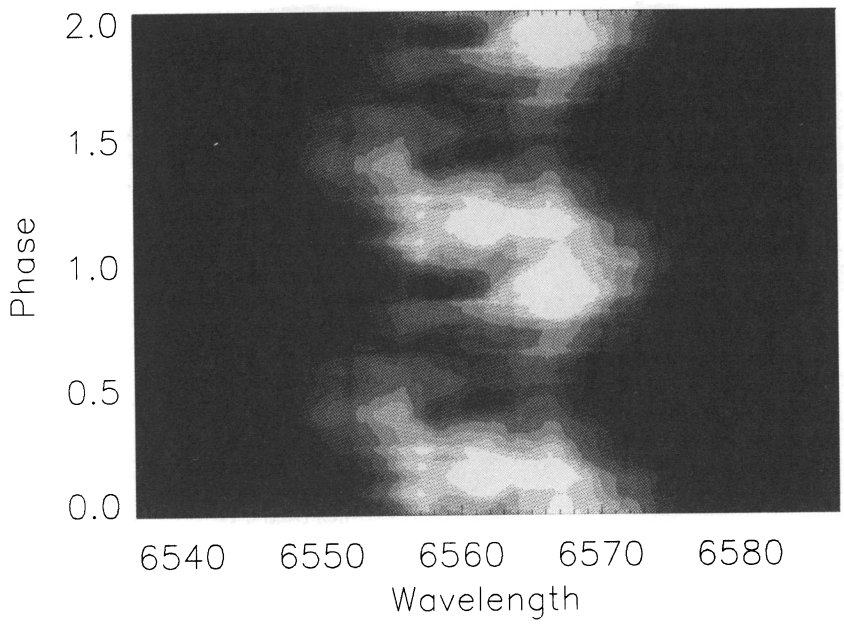

FIG. 3.—Excess Hα profiles (FK Com minus the standard) are shown vs. rotational phase, with wavelength increasing to the right and phase increasing upward. The data are repeated for phases 1.0–2.0. Intensity is linearly proportional to the flux. Data were interpolated linearly in phase to produce this pseudo-trailed spectrogram. Note the modulation with rotation in the velocity of the wings.

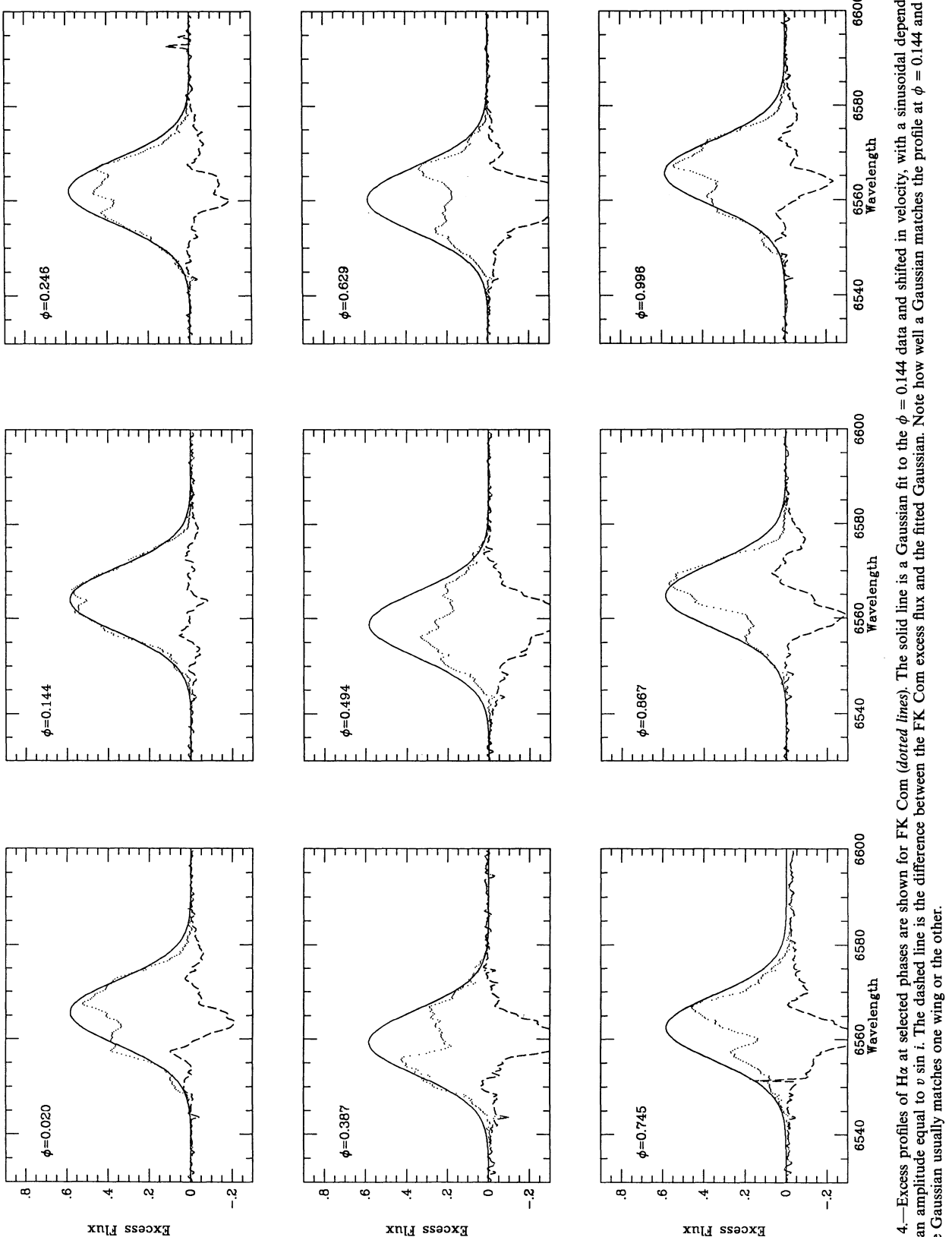

FIG. 4.—Excess profiles of Hα at selected phases are shown for FK Com (*dotted lines*). The solid line is a Gaussian fit to the $\phi = 0.144$ data and shifted in velocity, with a sinusoidal dependence having an amplitude equal to $v \sin i$. The dashed line is the difference between the FK Com excess flux and the fitted Gaussian. Note how well a Gaussian matches the profile at $\phi = 0.144$ and also how the Gaussian usually matches one wing or the other.

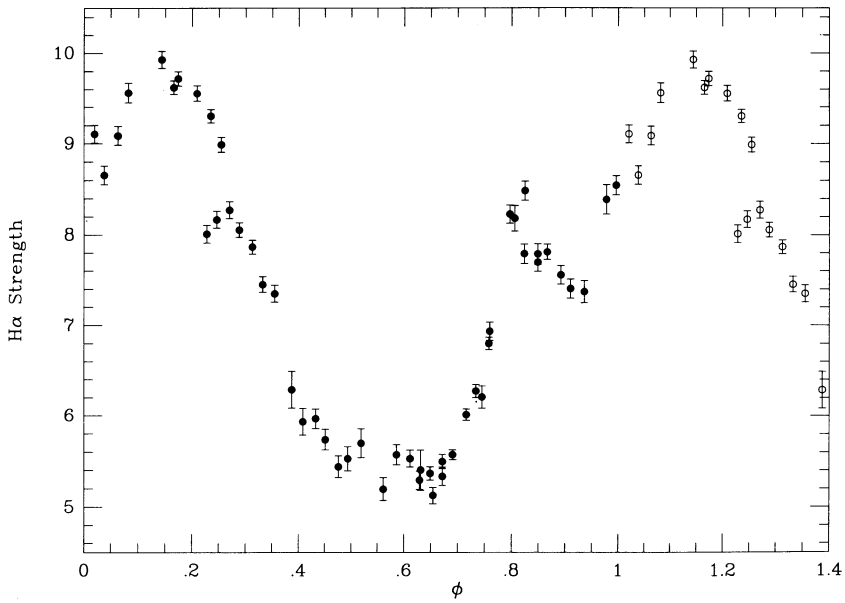

FIG. 5.—Hα excess strength is shown vs. rotational phase. Error bars of 1 standard deviation are shown, and open circles are data repeated at $\phi + 1$. Compare this with Fig. 2*a* to see how the maximum Hα strength corresponds to minimum brightness.

beginning at phase 0.35 and extending to phase 0.8. The outer wavelength limits of the blob are flanked by intermittent emission ridges (not apparent in the scaling of Fig. 6), separated by about $2v \sin i$. The corresponding image for Hγ (not shown) is similar to that of Hβ.

At first glance there appear to be substantial differences from Hα and the higher Balmer lines. For instance, when Hα shows nearly Gaussian excess emission, the other Balmer lines do not. Yet the strengths, centroids, and wings behave similarly. In fact, the *changes* in Hα strongly parallel the changes in other Balmer lines. If the Gaussian fit at phase 0.144 is subtracted from all the Hα excess profiles (after shifting in radial velocity), the resulting phase image looks nearly like the one for Hβ. The difference between Hα and Hβ is probably an optical depth effect, Hα being the thickest and showing the most emission. If we could observe pure emission from these lines, the Balmer decrement would be indicative of the temperature and density. The strength of Hβ goes to zero (that is, similar to an inactive star), while Hα remains strong, so we are not observing unadulterated emission from a volume of hot gas—we have radiative transfer or obscuration effects occurring. If we consider only the high end of the relationship where $W(\mathrm{H}\beta) > 1$ Å (when Hα is near Gaussian and Hβ has no excess absorption), then the ratio $W(\mathrm{H}\alpha)/W(\mathrm{H}\beta)$ ranges from 6 to 8 or, in terms of flux,

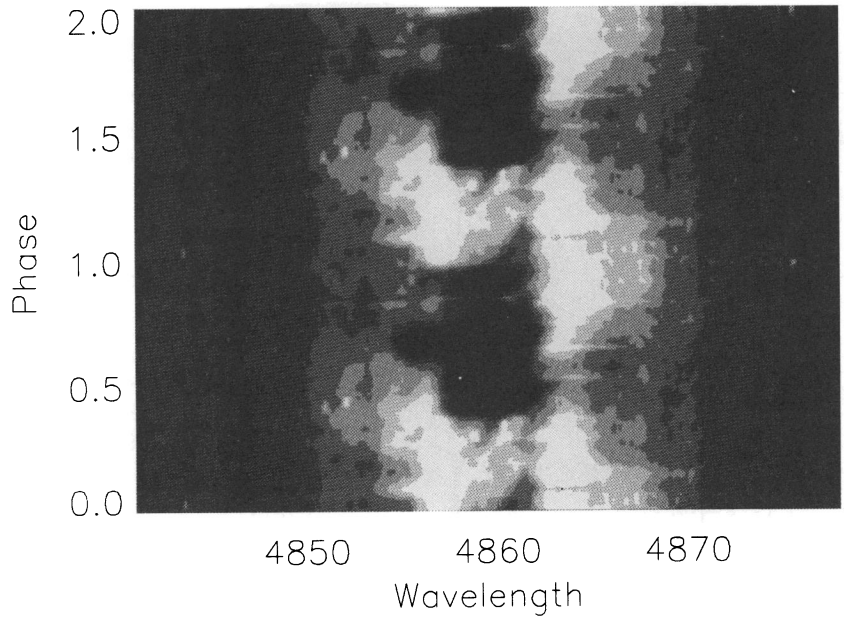

FIG. 6.—Hβ excess flux is shown vs. rotational phase in the same manner as Hα in Fig. 3. Note the strong excess absorption beginning at $\phi = 0.35$. An image made from the difference between the Hα excess and a Gaussian (see Fig. 4) looks very similar to this Hβ image.

from about 7 to 9. In the Sun, flares have a ratio (in flux) of 1 or less; plage, of less than 2, and prominences, of more than 5. The Balmer emission in FK Com, based on this comparison, seems to be indicative of extended, low-density material similar to a solar prominence.

There are two gross aspects of the Hα line: the large width and the velocity variation of the centroid. The large width could be due to corotating material extended to several stellar radii (Ramsey et al. 1981). In this case, the velocity variations would be explained by a longitudinally asymmetric distribution of matter. Based on close inspection of the velocity and phase behavior of Hα and other lines (see the following sections), it is our hypothesis that there is only mildly extended high-latitude material which causes the strong absorption component in the Balmer lines as it rotates into view. This is consistent with the minimum emission strength occurring slightly later than the maximum approaching line velocity and a velocity amplitude near $v \sin i$.

3.3. Ca II *Lines*

The lines of Ca II in our spectra, λλ8498 and 8542 of the infrared triplet, and the H and K lines in the near-ultraviolet, all show excess emission. Their strengths correlate well with those of Hα, and show the absorption component from phase 0.4 to phase 0.8. They do not, however, show any sign of modulation in centroid. The Ca II lines are all narrower than the Balmer lines, being only 300–400 km s^{-1} broad at the base. The uniformity of the Ca II line wings has been seen in RS CVn stars while at the same time the wings of Hα were highly variable (Buzasi, Ramsey, & Huenemoerder 1992a, b, c). Sample profiles are shown in Figure 7, where we can compare the widths of Ca II lines to each other and to Hα and Hβ, after scaling all multiplicatively to the same central height.

3.4. He I

The He I D3 line always shows substantial excess absorption and generally has emission wings. Both components are variable. Sample profiles are shown in Figure 8. There is much more structure in the variation with phase than was seen in Hα, although the basic form is similar to that shown in Figure 5. The He line is very weak or absent in inactive stars' spectra. It arises from a lower atomic level which is about 21 eV above ground, requiring substantial extreme ultraviolet flux, if it is populated radiatively or by photoionization and recombination. In the Sun, He I D3 is seen as a thin emission layer just above the limb, *except* under coronal holes (Zirin 1975). Zirin (1975) presented a photoionization-recombination model to explain the solar He I D3, with the ionizing flux coming from the corona. If the layer of excited helium were thick enough, it would be apparent in absorption when one looked through it at the photosphere.

A substantial nonuniform shell of excited He I would explain the He I D3 profiles of FK Com very well. The profile is that of a rotationally broadened absorption line with limb brightening. The separation of the emission wings seen in Figure 8 is about $2.2v \sin i$, consistent with a slightly extended shell. The variability represents a projection of a nonuniform corona onto the photosphere. In the simplified case of one "blob" of excited helium, one would first see blue-wing emission, which then decreases and changes to the central absorption, reaching a maximum one-quarter phase later. One-quarter rotation after that, the region would be seen on the receding limb and produce a red-wing emission bump. We have looked for such

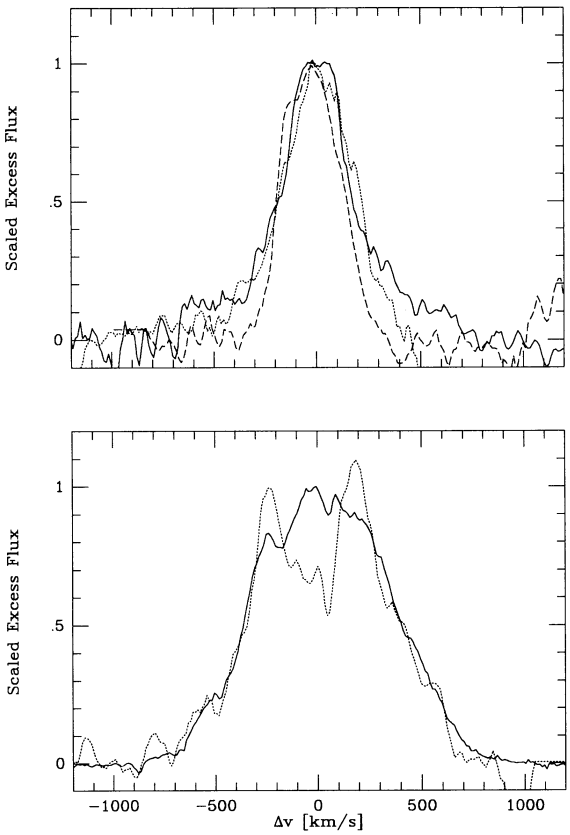

FIG. 7.—Ca II (*top*) and Balmer excess (*bottom*) lines profiles are compared after scaling to the same central height. Of the Ca II lines, the solid line is Ca II H, the dotted line is Ca II K, and the dashed and narrowest line is λ8542 of the infrared triplet. In the lower panel, Hα is the solid line and Hβ is shown as a dotted line. All are taken from the same spectrum. It is obvious that the Balmer lines are similar in their extreme width, and that the calcium lines are narrower. The extended wings of the Ca II H and K lines may be due to a spectral type mismatch in the standard; these wings are very strong in cool stars.

simple behavior in the data via cross-correlation techniques but have not found significant peaks. This is evidence of more complicated structure which masks correlations of individual blobs. We have successfully fitted individual line profiles with an ad hoc spatial distribution of excited helium, within a parameterized limb-darkening/limb-brightening law. However, to take advantage of the rotational phase information to derive a self-consistent map, sophisticated iteratives schemes are needed.

FK Com is a known X-ray source, having been detected by *Einstein* (Walter 1981). There is thus evidence of a corona as a source of the He-ionizing radiation. In further support of the photoionization-recombination model for He in FK Com, there is also a strong emission line near 3889 Å. It is unlikely that this is a Balmer line, H8, since Hε and Hγ are not as strong, or as narrow. It is more likely He I λ3889, which is a transition to the metastable ground state of orthohelium. It appears in emission only because there is not enough flux in the continuum from the star; that is, the source function of the recombining helium shell is always greater than that of the photosphere behind it. The data in this spectral region are rather noisy, but the line does not appear to be a CCD flaw, as it is wide and does not appear in neighboring orders, in contrast to an obvious CCD flaw just blueward of Ca K. A dis-

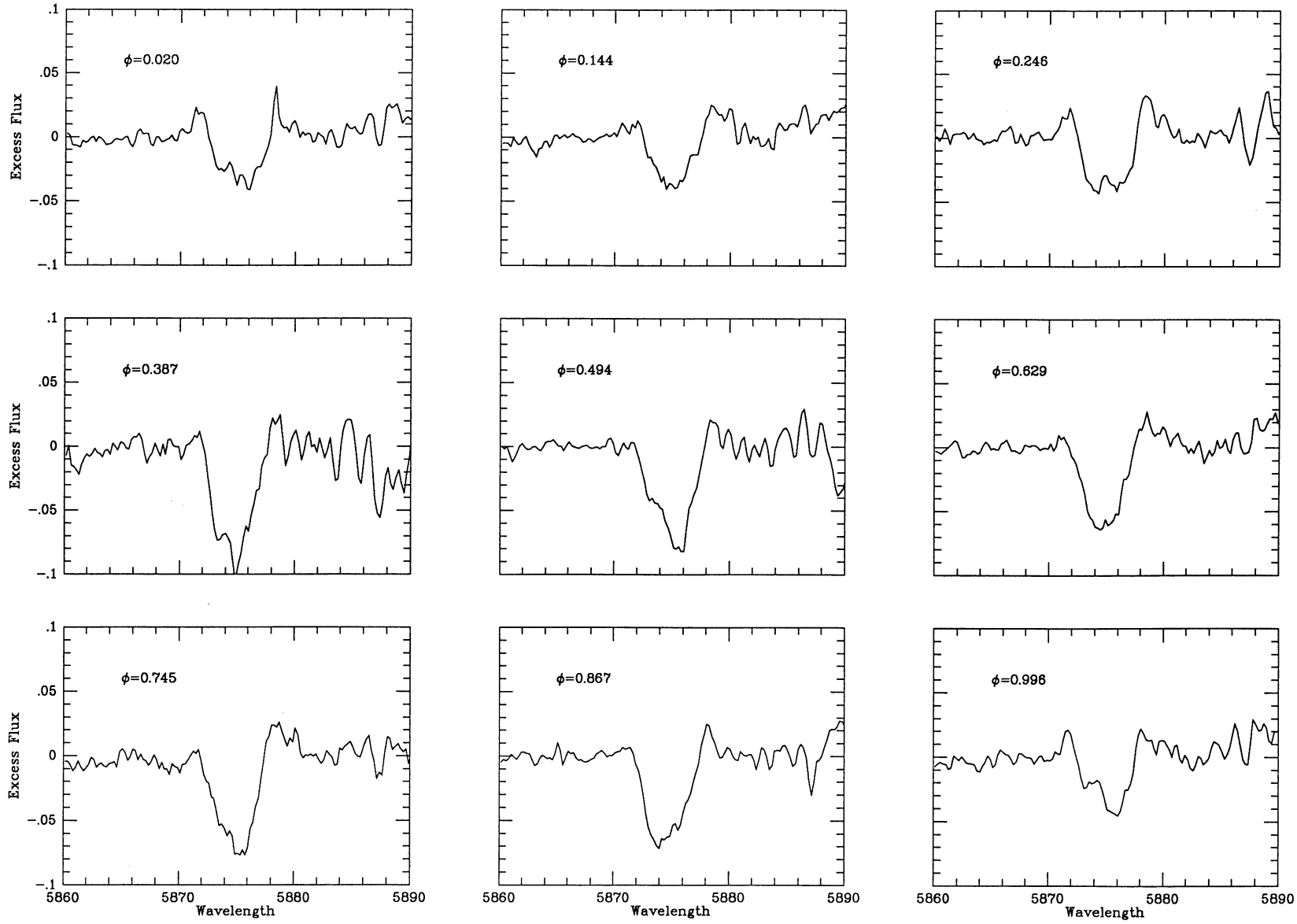

FIG. 8.—He I D3 excess profiles are shown for representative rotational phases. Since there is no appreciable line in an inactive star, particularly when its spectrum is artificially rotationally broadened, these are essentially the same as the intrinsic profiles. Note the emission wings and the broad absorption, characteristic of a limb-brightened absorption line.

crepant wavelength is troublesome, since the line occurs in our spectra at 3981 Å. In velocity space, it is coincident with the red emission bump on He D3 at the same phase, but there is no corresponding blue bump. It is likely that the wavelength solution is in error, because the thorium-argon spectrum was weak here, and there is no adjacent order on the blueward side to allow interpolation. It is fortunate that the Ca K line, in the same spectral order but at the other end, has a good wavelength. Additional higher quality spectra are needed to test the helium recombination hypothesis. It is also important to obtain He I λ10830 spectra, since this is the fundamental transition of orthohelium. X-ray observations, important to determining the amount of ionizing flux, have recently been made with *ROSAT*.

The He I lines may offer our best hope for understanding the structure and energetics of the FK Com atmosphere. It is likely that their behavior and origin can be better understood and modeled than those of the Balmer lines.

4. ULTRAVIOLET CHROMOSPHERIC AND TRANSITION REGION LINES

FK Com has been previously observed in the ultraviolet with *IUE* (Bopp & Stencel 1981). In doing flux-flux correlations in active stars, it is necessary to have contemporaneous data to avoid changes in activity level between observations. Hence, we obtained *IUE* spectra during and after our visual data run. The UV part of the spectrum contains lines from the low chromosphere (CR), such as Mg II λ2800, to the upper CR (O I λ1302), to the transition region (TR; C IV λ1540). This also represents an increasing temperature sequence. In Figure 9 we show the dependence of Mg II and C IV on rotational phase. It is apparent that Mg II decreased in strength in the 70 days following the contemporaneous observations. C IV, which is the strongest of the TR lines, does not obviously show such a trend. It is difficult to determine any degree of rotational modulation in the UV line strengths in these sparse data. Since Hα is so strongly modulated with phase, we pair each of the contemporaneous points with the Hα point nearest in phase and show the resulting flux-flux correlation in Figure 10. Mg II shows a clear direct relation with Hα, but the C IV does not. If this is a reflection on the region of formation, one might expect the correlation to disappear gradually as one selects higher temperature lines. However, the CR and TR lines from all the data in the short-wavelength *IUE* spectra correlate quite well with each other (Fig. 10*c*) and, by inference, not with Hα or Mg II. We see no rotationally coherent behavior in any CR or TR lines other than Mg II. The emission from higher temperature regions may represent transient features, such as flares, or a small number of regions of small geometric scale which can form or decay quickly, while the Hα and Mg II may represent the global structure of the active regions. Flaring is partially substantiated by the higher TR fluxes at a given CR flux, as seen in Figure 10, but there is no obvious signature in the optical data. Although Hα and Mg II have different formation mechanisms, they are the most optically thick lines in the present data. Therefore, we expect them to be more sensitive to the extended structures, while the other lines are too optically thin to show the same regions. The emission-region structure apparently changes quite rapidly with height. Better time resolution of UV chromospheric and transition region lines is needed to derive this structure.

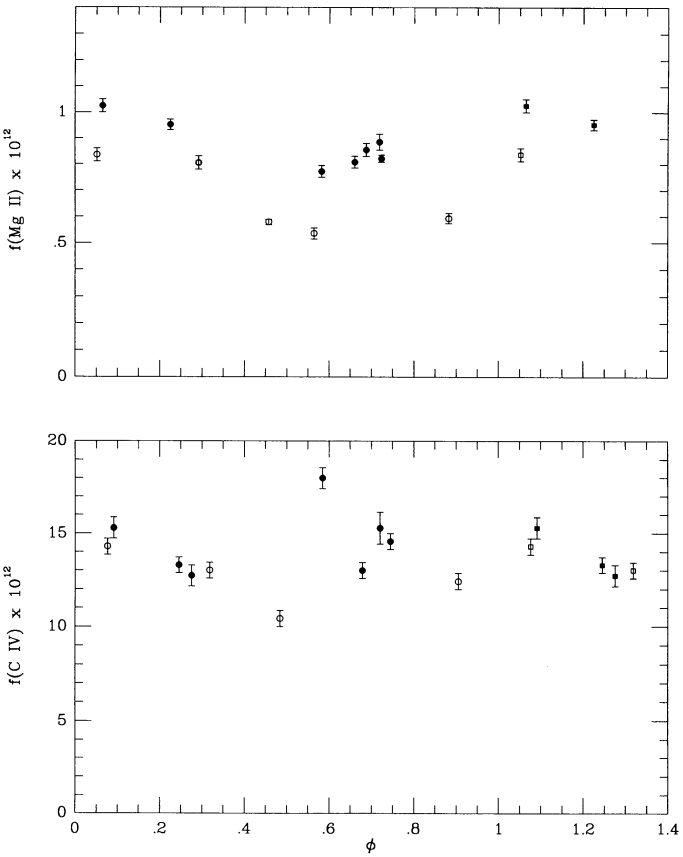

FIG. 9.—Two representative ultraviolet line fluxes are shown vs. rotational phase. The top panel shows Mg II, the bottom C IV. Filled symbols represent data taken contemporaneously with the visual spectra. Open symbols denote data taken about 70 days later. Mg II, a low-temperature chromospheric line, shows possible modulation and systematic changes in the interval between the two data sets. The C IV line, formed at temperatures characteristic of the solar transition region, does not show the same behavior.

5. FK COMAE AMONG THE ACTIVE STARS: FLUX-FLUX RELATIONS AND ROTATION

The solar activity paradigm has long been in use for interpretation of phenomena in cool stars, ranging from pre–main-sequence stars, active dwarfs, and dwarf binaries (BY Dra stars) to evolved binaries (RS CVn stars). Phenomena which have been invoked to explain photometric modulation, various emission lines, and X-ray emission are cool spots, plage, prominences, chromospheres, transition regions, and coronae, in analogy to the Sun. Rapid rotation due to youth or tidal coupling is the common feature among the diverse mix of active stars. However, the details of the conversion of magnetic energy into thermal heating are still a subject of intense investigations. As extreme cases often establish the rule or its exceptions, FK Com has been a natural target. Its rotation rate is extreme, and it lacks a companion. This leads to the hypothesis that FK Com is a recently coalesced binary. This scenario puts FK Com in an interesting and short-lived evolutionary state.

Previous published values using surface fluxes or distance-dependent parameters have had to use fairly uncertain quantities. Given the current work and that of others, we can improve some of these. Eggen & Iben (1988, 1989) have identified FK Com as a member of the old disk group, HR 1614. From their Figure 4, M_V is estimated to be about 1.5, which,

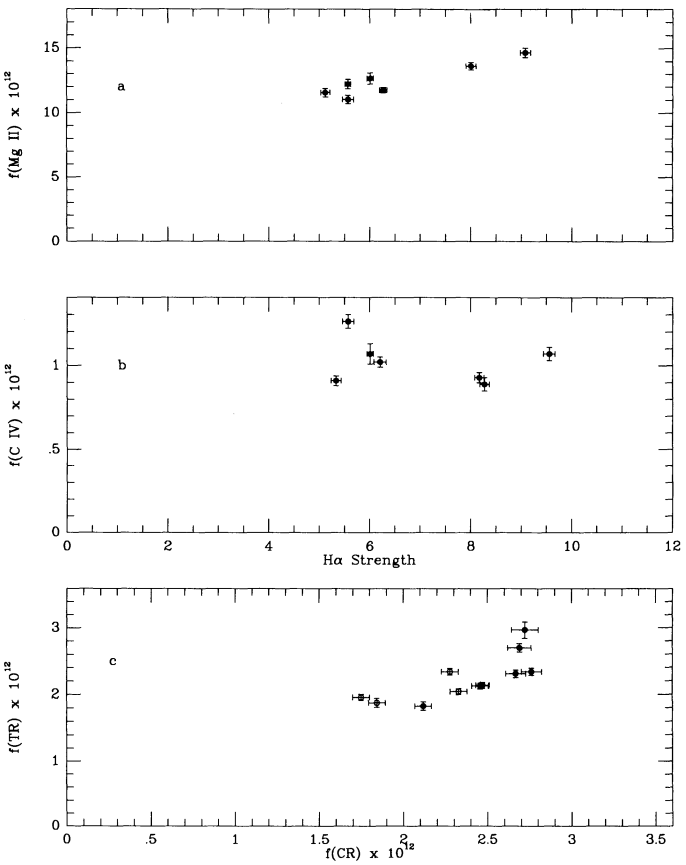

FIG. 10.—Flux-flux relations are shown for UV and optical lines. (*a*, *b*) The top and middle panels show Mg II and C IV vs. Hα. There is a correlation between Mg II and Hα, but none is seen for C IV and Hα. Only contemporaneous data are shown, pairing points closest in phase, generally taken within the same rotation. (*c*) The bottom panel shows the relationship between the fluxes for transition region (TR) and chromospheric (CR) lines from the short-wavelength region of *IUE*; these are weakly correlated. The variations are not correlated with Hα or rotational phase, since C IV dominates the TR flux and shows no such correlations.

when combined with the mean visual magnitude of 8.2, yields a distance of 219 pc. As mentioned in § 3.1, Eggen & Iben's work also indicates an approximate mass and limit on the inclination. Adopting the median implied sin i of 0.9 gives a radius of $8.6 \pm 0.2 R_{\odot}$. Applying this along with the visible flux at Earth and a surface flux calculated from the Barnes-Evans relationship (Barnes, Evans, & Moffett 1978), using $(V - R) = 0.75$ from Bianchi & Grewing (1985), gives a distance of 215 ± 5 pc, which we will adopt. The Barnes-Evans visual and red surface fluxes can also be used to calculate the blackbody equivalent effective temperatures, and give $T_{\rm eff} = 5800$ K. This is consistent with the Bianchi & Grewing value of 6000 K estimated from *IUE* continua. We can thus estimate a bolometric luminosity of 2.9×10^{35} ergs s^{-1}. Hence, we now have independent, consistent, and believable fundamental parameters for FK Com.

There is one *Einstein* IPC flux for FK Com, 0.25 counts s^{-1}. Using the conversion factor from Cruddace & Dupree (1984) yields an X-ray luminosity of $L_x = 2.8 \times 10^{31}$ ergs s^{-1} With the above values, we find $L_x/L_{\rm bol} = -4.0$, as compared to the previous value of -3.5 from Walter (1981). (*ROSAT* observations made in 1992 January will further improve the X-ray flux and also provide needed X-ray spectral information.)

We may now update published correlations with these improved parameters. On the $L_x - v \sin i$ correlation (Cruddace & Dupree 1984; Pallavicini 1989), FK Com is extreme, but consistent with the mean relationship. It lies within the scatter of the fitted function, and lies at the top of the RS CVn maximum in L_x and at higher velocities (see Cruddace & Dupree 1984, Fig. 4), far above the contact binaries of similar rotational velocity. However, if we look at the $L_x/L_{\rm bol}$–log P relationships, we see that FK Com lies well below the RS CVn stars (Walter & Bowyer 1981) and among F8–G5 dwarfs (Walter 1981). Its $L_x/L_{\rm bol}$ is in fact about 5 times lower than that of the lowest RS CVn near the same period, AR Lac, a well-studied coronal source of *lower* $v \sin i$ (White et al. 1987; Bopp & Stencel 1981). Bopp & Stencel's graphs (their Fig. 2) showed a UV excess and an X-ray deficiency as compared with RS CVn stars. Their points for FK Com need to be adjusted, however, according to our improved distance and radius. The result of this is to shift the FK Com point down and to the left on the UV-UV line flux correlations, with the result that it essentially coincides with the RS CVn points, as denoted by the linear relation and the mean point for HR 1099 and UX Ari. The X-ray point, however, remains deficient, being more than an order of magnitude below the RS CVn systems. FK Com lies at the upper extreme in the active star Mg II flux versus $(B - V)$ relationship shown by Zwaan (1986) [for FK Com, log $F_{\rm Mg\,II} = 7.4$ and $(B - V) = 0.88$], but the Bopp & Stencel results show that the other UV lines are equally enhanced. Thus, we are left with the conclusion that relative to other active giants, and for its bolometric luminosity, FK Com has "normal" UV lines but is very deficient in X-rays. Resolution of this discrepancy will require further X-ray data. Perhaps the X-rays are absorbed by circumstellar material. The strong Balmer emission in conjunction with the high Balmer decrement is also supportive of an excess of extended, low-density matter. Based on our data and the existing X-ray measurement, we predict that the X-ray flux not only will vary with rotation but will change in hardness as obscuring material is carried through the line of sight.

6. SUMMARY AND CONCLUSIONS

We have provided a wealth of data, numerous correlations, and some interpretations regarding the nature of FK Com. It has dark spots (apparent from photometry and spectroscopy), has no companion though rotating near breakup velocity, and is very active. While the Balmer decrement is indicative of extended matter, the velocity behavior implies confinement within 1 stellar radius from the rotation axis. While the He D3 absorption line indicates substantial X-ray or extreme UV flux, the star is underluminous in X-rays. The lower chromospheric lines' fluxes are modulated by rotation, but higher CR and TR lines are not; both are consistent with the activity-rotation relationship extrapolated from RS CVn stars. Recently obtained X-ray spectra with *ROSAT* should help to understand the X-ray deficit, which could be due to excess absorption by circumstellar material. While it is too early to draw firm conclusions, FK Com's conspicuous absence from the *ROSAT* wide-field camera catalog of sources (Pounds et al. 1992) also suggests substantial obscuration. Identification of further bona fide members of the FK Comae "class" are desperately needed in order to quantify the evolutionary state of this purported coalesced binary star system.

We are grateful to Sam Barden and Sidney Wolff at NOAO for their continuing support of the Fiber Optic Echelle spectrograph, on loan from Penn State. The research decribed in this paper was carried out by the Jet Propulsion Laboratory, California Institute of Technology, under a contract with the National Aeronautics and Space Administration, and by the Pennsylvania State University under NSF grant AST8919205 and NASA grant NAG5563. H. L. N. thanks Michael Zeilik for a copy of the SPOT starspot modeling program and for several useful discussions on its use. The APT photometry reported here was supported by a AAS Small Research Grant to H. L. N.

REFERENCES

Barnes, T. G., Evans, D. S., & Moffett, T. J. 1978, MNRAS, 183, 285
Bianchi, L., & Grewing, M. 1985, A&A, 283, 200
Bopp, B. W., & Stencel, R. E. 1981, ApJ, 247, L131
Budding, E. 1977, Ap&SS, 48, 287
Budding, E., & Zeilik, M. 1987, ApJ, 319, 827
Buzasi, D., Ramsey, L. W., & Huenemoerder, D. P. 1992a, ApJ, submitted
———. 1992b, ApJ, submitted
———. 1992c, ApJ, submitted
Chugainov, P. F. 1976, Izv. Krymsk. Astrofiz. Obs., 54, 89
Cruddace, R. G., & Dupree, A. K. 1984, ApJ, 277, 263
Dorren, J. D., & Guinan, E. F. 1990 ApJ, 348, 703
Dorren, J. D., Guinan, E. F., & McCook, G. P. 1983, Inf. Bull. Var. Stars, 2276, 1
Eggen, O. J., & Iben, I. 1988, in ASP Conf. Ser., Vol. 1, Progress and Opportunities in Southern Hemisphere Optical Astronomy, ed. V. M. Blanco & M. M. Phillips (San Francisco: ASP), 239
———. 1989, AJ, 97, 431
Genet, R. M., Boyd, L. J., Kissell, K. E., Crawford, D. L., Hall, D. S., Hayes, D. S., & Baliunas, S. L. 1987, PASP, 99, 617
Holtzman, J. A., & Nations, H. L. 1984, AJ, 89, 391
Huenemoerder, D. P., Buzasi, D. L., & Ramsey, L. W. 1989, AJ, 98, 1398
McCarthy, J. K., & Ramsey, L. W. 1984, ApJ, 283, 200
Merrill, B. 1948, PASP, 60, 382
Pallavicini, R. 1989, Astron. & Astrophys. Rev., 1, 177
Pounds, K. A., et al. 1992, in preparation
Ramsey, L. W., & Huenemoerder, D. P. 1986, Proc. SPIE, 621, 282
Ramsey, L. W., Huenemoerder, D. P., Buzasi, D. L., & Barden, S. C. 1987, in Proc. Fifth Cambridge Workshop on Cool Stars, Stellar Systems, and the Sun, ed. J. L. Linsky & R. E. Stencel (New York: Springer-Verlag), 515
Ramsey, L. W., Nations, H. L., & Barden, S. C. 1981, ApJ, 251, 101
Rosenthal, S. M. 1986, Master's thesis, Pennsylvania State Univ.
Walter, F. M. 1981, ApJ, 245, 677
Walter, F. M., & Basri, G. 1982, ApJ, 260, 735
Walter, F. M., & Bowyer, S. 1981, ApJ, 245, 671
Walter, F. M., Neff, J. E., Bopp, B. W., & Stencel, R. E. 1984, in Proc. Third Cambridge Workshop on Cool Stars: Stellar Systems, and the Sun, ed. S. L. Baliunas & L. Hartmann (New York: Springer-Verlag), 279
White, N. E., Shafer, R., Parmar, A. N., & Culhane, J. L. 1987, in Proc. Fifth Cambridge Workshop on Cool Stars, Stellar Systems, and the Sun, ed. J. L. Linsky & R. E. Stencel (New York: Springer-Verlag), 521
Zirin, H. 1975, ApJ, 199, L63
Zwaan, C. 1986, in Proc. Fourth Cambridge Workshop on Cool Stars, Stellar Systems, and the Sun, ed. M. Zeilik & D. Gibson (Berlin: Springer-Verlag), 19